Article

Mathematical Modelling of Muña Leaf Drying (*Minthostachys mollis*) for Determination of the Diffusion Coefficient, Enthalpy, and Gibbs Free Energy

Reynaldo J. Silva-Paz *, Dante K. Mateo-Mendoza and Amparo Eccoña-Sota

E.P. Ingeniería de Industrias Alimentarias, Facultad de Ingeniería y Arquitectura, Universidad Peruana Unión, Lima 1546, Peru
* Correspondence: rsilva@upeu.edu.pe; Tel.: +51-957805238

Abstract: In Peru, there are more than four thousand plants with medicinal properties, including muña, which helps digestion and improves health. The way to preserve these plants is drying up. The objective of this research was to investigate the coefficient of diffusion, enthalpy, and Gibbs free energy in the drying kinetics of muña leaves. Different pretreatments were carried out on the samples (without pretreatment, as well as treated by immersion in 1% ascorbic acid and bleaching at 60 °C for 30 s), and they were dehydrated at three temperatures (40, 50, and 60 °C). The drying kinetics were modeled using eight mathematical models to represent the drying curve. The water content was reduced by the drying process. The logarithmic model was selected, as it showed the best fit to represent the drying kinetics of the muña. Activation energy values were similar between treatments ($p > 0.05$). The increase in temperature decreases the enthalpy and entropy and increases the Gibbs free energy with the effective diffusion coefficient. The drying kinetics allows one to determine the drying time for the storage of the product and the thermodynamic properties for the design of the equipment.

Keywords: kinetics; drying; models; muff; thermodynamics

1. Introduction

The leaves of the muña plant possess significant medicinal properties and are utilized as an analgesic, antispasmodic, and antiseptic against respiratory diseases and rheumatism. These health benefits can be attributed to the leaves' high levels of antioxidants, calcium, and phosphorus, which are vital for maintaining bone health and, in some instances, for developing nutraceutical products [1,2]. In a study by Paw-er-Pucurimay et al. [3], the medicinal use of muña leaves was investigated to analyze the effects of alkaloids and phenols. As the leaves of medicinal plants have a high-water content, which can lead to metabolic activity increases and physical and chemical changes during storage, it is essential to decrease the water content through a process that preserves the medicinal leaves' quality and functionality after harvest.

Muña (*Minthostachys mollis*) is a herb that grows in the Andes mountain range at elevations between 2500 and 3500 msnm. It is found in the Andean departments of Junín, Ayacucho, and Cuzco, typically sprouting its first leaves in September [1]. The herb is consumed by older adults in Peru, with consumption accounting for 5.8% of its usage in 2017 [4,5]. It is often used to alleviate digestive and respiratory pain [6], or it is applied as an insect repellent for potato storage due to its high terpenoid content in essential oil [7]. Despite these benefits, consumption is limited due to the lack of knowledge of its medicinal properties and a lack of diversification.

There are various methods to preserve the nutritional and quality attributes of food. One of them is drying, which allows one to preserve the quality and stability of food by reducing water activity, reducing its moisture content to prevent deterioration during

storage. In addition, this process increases the content of vitamins, minerals, and fiber, converting foods into functional products [8]. Drying also decreases the weight and volume of food, which reduces transportation and storage costs.

The temperature of the drying air plays a critical role in the drying process of leaves, and it depends on the heat sensitivity of the active components in the sheet and the moisture migration rate. Higher temperatures facilitate faster drying; however, it is important to choose the temperature carefully to prevent burns on the surface of the leaves [9]. Although the most common approach for drying leaves is direct or indirect solar energy drying, this method has several drawbacks, including lack of process control, potential issues with the final product's quality, and concerns regarding microbiology and food safety. Other techniques, such as hot air drying [10], conventional microwave drying [11], and osmodehydrofreezing [12], have been proposed as alternative methods to preserve the quality of the final product.

For process control and production of high-quality products, mathematical modeling and simulation of the drying curve is important. This information is valuable to evaluate the drying kinetics, as well as to analyze variables and to optimize the drying parameters. These processes allow one to minimize the damage to the quality of the product, to reduce excessive energy consumption, and to prevent excessive wear of the drying equipment. In addition, these benefits contribute to improved performance [8,13]. Activation energy is the energy required for a chemical reaction or physical process to occur. In the case of leaf drying, knowing the activation energy is important to select the optimal temperature and time to dry the leaves efficiently. If the activation energy is too high, the drying process will be slow and expensive. If it is too low, it can cause a degradation of the quality of the sheets. Some of the empirical equations generally used to study and model food drying kinetics are Midilli, Newton, Page, Peleg, Henderson–Pabis, modified Page, logarithmic, Wang, Singh, and exponential [14]. The aim of this research was to assess how drying temperature affects the kinetics, diffusion coefficient, activation energy, enthalpy, entropy, and Gibbs free energy in muña leaf drying.

2. Materials and Methods

2.1. Raw Material

Muña plants (30 ± 2 cm tall) were collected in January 2019 in the department of Junín, at 3300 msnm (12°04′00″ S, 75°13′00″ W). Leaves of 2 ± 0.5 × 1 ± 0.2 cm, which were greenish, without brown or broken spots, were selected. These were placed on kraft paper and stored in polypropylene bags at room temperature for 24 h. Moisture was determined using a digital moisture balance in a dry basic configuration (Pesacon MX-50, Space and Time, Lima, Peru).
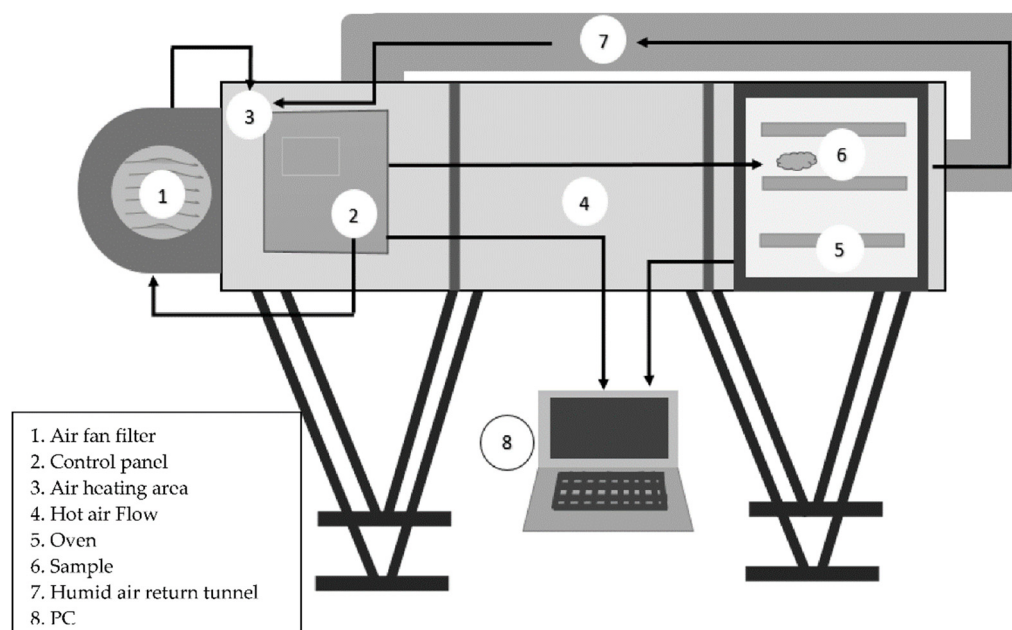
2.2. Raw Material Conditioning

For the conditioning of the leaves (Humidity: 78.5%) before the drying process, three pre-treatments were chosen: without pre-treatment (SB), leaves treated by immersion in a 1% ascorbic acid solution for 30 s at 40 °C (BAA), and leaves subjected to a bleaching process at 60 °C for 30 s (B60). For the last two treatments, we worked with leaves at a liquid ratio of 1:10, and, in this process, the samples were cleaned with adsorbent paper to remove excess water to submit them to the drying process [15].

2.3. Drying Process

This process was carried out in a tray tunnel dryer (Space and Time, HSB01, Lima, Peru) that controls the speed and temperature of the inlet air, which is heated through electrical resistances (Figure 1). Three temperatures were used in the study of drying kinetics: 40, 50, and 60 °C, and each treatment was carried out in triplicate, the drying air flow was kept constant at 2.0 ± 0.2 m/s, and the relative humidity input was 68.08 ± 0.60%. The leaves were placed in a thin layer per tray, and the initial weight of each treatment was recorded. Weight variation was measured on an analytical balance, with an accuracy of

$\pm$0.001 g at 30-min time intervals, and drying time was completed until constant weight was reached [10].

1. Air fan filter
2. Control panel
3. Air heating area
4. Hot air Flow
5. Oven
6. Sample
7. Humid air return tunnel
8. PC

Figure 1. Diagram of the convective tray dryer tunnel.

2.4. Mathematical Models

The drying process, in terms of product quality and operating costs, is based on the prediction of the drying rate with the help of suitable mathematical models. Mathematical models of drying kinetics can be classified into three groups: empirical exponential, empirical non-exponential, and Fick's second law, or else diffusional models were used. Modeling attempts to establish a real model to simplify and delimit the process. Table 1 shows the mathematical models used to model the drying kinetics of muña leaves [14].

Table 1. Mathematical models that describe drying kinetics.

Model Name	Model Equation	Equation
Page	$MR = \exp(-k \cdot t^n)$	(1)
Modified Page	$MR = \exp(-k \cdot t)^n$	(2)
Midilli	$MR = a \cdot \exp(-k \cdot t^n) + b \cdot t$	(3)
Lewis	$MR = \exp(-k \cdot t)$	(4)
Wang and Singh	$MR = 1 + (a \cdot t) + (b \cdot t^2)$	(5)
Logarithmic	$MR = a \cdot \exp(-k \cdot t) + c$	(6)
Peleg	$MR = (1 - t)/(k_1 + (k_2 \cdot t^2))$	(7)
Henderson and Pabis	$MR = a \cdot \exp(-k \cdot t)$	(8)
Moisture ratio	$MR = (w_t - w_e)/(w_o - w_e)$	(9)

Where: a, b, c, k, n are constants of the kinetic models, MR is moisture ratio, w_t is the real-time moisture content (g water/g sample), w_o is the initial moisture content (g water/g sample), and w_e is the equilibrium moisture content (g water/g sample).

2.5. Activation Energy and Thermodynamic Properties

To calculate the effective diffusivity coefficient, Fick's second law was used, which adequately describes the diffusivity phenomena in the mass transfer in the sample during drying until reaching equilibrium. Considering that muña sheets are the closest thing

to an infinite sheet, the mass transfer is one-dimensional with long drying times. The mathematical model is expressed in Equation (10):

$$\ln(MR) = \ln\left(\frac{8}{\pi}\right) - \left(\frac{\pi^2 D_{eff}}{4L_0^2}\right)t \tag{10}$$

where: D_{eff} is effective diffusivity coefficient (m/s^2), and L_0 is the semi-thickness of the sheet to be dried (m).

D_{eff} was determined through the graph of $\ln(MR)$ versus time of the experimental data by means of the slope $\left(\frac{\pi^2 D_{eff}}{4L_0^2}\right)$ of Equation (10).

In general, the effective diffusivity coefficient of water in foods depends predominantly on the drying temperature and shows an Arrhenius-type trend. To evaluate the dependence of the empirical constants as a function of temperature, the linearized Arrhenius equation (Equation (11)) was used. The kinetic parameters activation energy (E_a) and initial diffusion constant (D_0) were estimated from the slope and intercept of the graph $\ln(D_{eff})$ versus $1/T$ [16].

$$\ln\left(D_{eff}\right) = lnD_0 - \left(\frac{E_a}{R}\right)\left(\frac{1}{Ta}\right) \tag{11}$$

where: D_{eff} is a rate constant to evaluate empirical constants, R is the universal gas constant (8.314 J/mol·K), E_a is the activation energy (kJ/mol), D_0 is the Arrhenius factor (m^2/s), and Ta is the absolute temperature (K).

Knowing the activation energy, the differential enthalpy (Equation (12)), the differential entropy (Equation (13)), and the Gibbs free energy (Equation (14)) were determined using the following equations [17]:

$$\Delta H^* = E_a - RT \tag{12}$$

$$\Delta S^* = R\left(lnD_0 - \ln\frac{K_B}{h_P} - \ln T\right) \tag{13}$$

$$\Delta G^* = \Delta H^* - T\Delta S^* \tag{14}$$

where: K_B is Boltzmann constant (1.38×10^{-23} JK^{-1}, the Planck constant is h_p (6.626×10^{-34} J·s), and T is the absolute temperature (°K).

2.6. Statistical Analysis

The goodness-of-fit of the proposed models for the drying kinetics was evaluated by means of statistical tests that include the squared sum error, SSE (Equation (15)); square root mean squared error, RMSE (Equation (16)), the coefficient of determination, R^2 (Equation (17)), and the mean square error (MSE, Equation (18)). This was accomplished by using the XLSTAT 2022 software. The lowest values of SSE and RMSE (≈ 0.0) and the highest values of the coefficient of determination r^2 (≈ 1.0) were considered as criteria to select the best fit between the models.

$$SSE = \frac{1}{N}\sum_{i=1}^{N}(MR_{e,i} - MR_{c,i})^2 \tag{15}$$

$$RMSE = \sqrt{\frac{1}{N} * \sum_{i=1}^{N}(MR_{pre,i} - MR_{exp,i})^2} \tag{16}$$

$$r^2 = 1 - \frac{\sum_{i=1}^{N}(MR - MR_{c,i})^2}{\sum_{i=1}^{N}(MR_{e,i} - MR_{c,i})^2} \tag{17}$$

$$\text{MSE} = \frac{1}{N} \sum_{i=1}^{N} (F_c - MR_{c,i})^2 \tag{18}$$

where: $MR_{e,i}$ is the experimental moisture content, $MR_{c,i}$ is the calculated moisture content, I is the number of terms, z is a constant number, c is the value given by the model, and N is the number of data.

3. Results and Discussion

3.1. Drying Kinetic Curves

In Figure 2 are the experimental curves of the drying of the muña leaves pretreated and subjected to three temperatures. All the curves showed a clear decreasing trend with the moisture ratio (MR), which decreased rapidly as the drying temperature of the air increased.
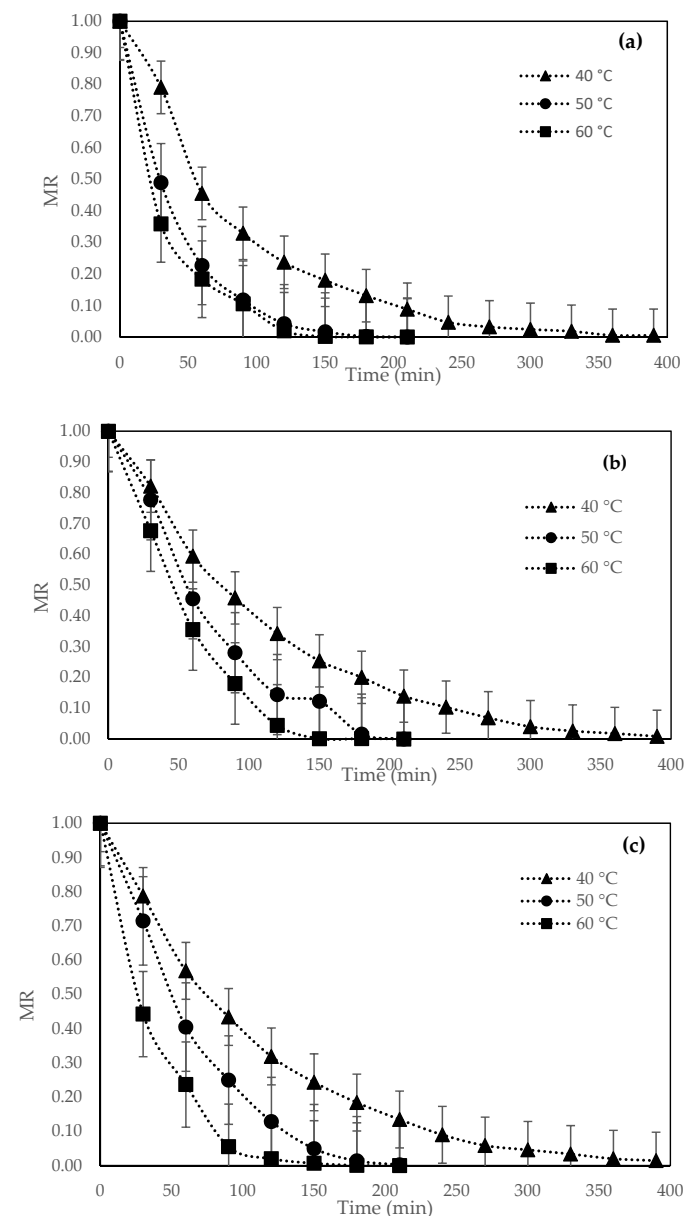
Figure 2. Variations of the moisture ratio (MR) as a function of time at different drying temperatures: (**a**) SB: without pretreatment, (**b**) BAA: immersion in a 1% ascorbic acid solution for 30 s at 40 °C, and (**c**) B60: bleaching process at 60 °C for 30 s ((**c**), adjusted to the logarithmic model).

It was observed that the drying time was shorter as the drying temperature increased; that is, the drying speed increased with the increase in the drying air temperature. The times were 480, 240, and 210 min at temperatures of 40, 50, and 60 °C, respectively. Therefore, increasing the temperature of the drying air considerably reduced the time required for the muña leaves to have a lower moisture content.

This phenomenon was confirmed by other researchers who studied the drying kinetics in other medicinal plants, for example, Martins et al. [18] in timbo leaves; this was also performed by Silva et al. [19] in genipapo, as well as Gasparin et al. [20] in Mentha piperita leaves. The effect of the temperature of the drying air on the reduction of the drying time of muña leaves can be attributed to the fact that the main cause of the drying process is the difference in vapor pressure between the product and the drying air. The vapor pressure difference increases with the increase in the temperature of the drying air [18].

At lower temperatures, the time required to remove water from the surface of the product is longer than at higher temperatures because, at lower temperatures, the contribution to the removal of water present on the surface is low. This behavior of shorter drying time at higher temperatures can be explained by the structure of the sheets, the drying conditions, the increase in mass transfer coefficients, and the increase in the vapor pressure gradient between the drying air and the air inside leaves [21,22].

3.2. Mathematical Modeling of Drying Kinetics

Eight drying models were used—Lewis, Page, modified Page, Henderson and Pabis, logarithmic, Midilli, Peleg, Wang, and Singh—to describe the drying kinetics of muña leaves during convective drying processes, with hot air used at 40, 50, and 60 °C. The model constants and statistical parameters R^2, SSE, MSE, and RMSE of the tests are shown in Tables 2–4. The highest values of R^2 and the lowest values of RMSE were selected as criteria for the accuracy of the fit.

The logarithmic model provided the best fit for all treatments during experimental drying at the three temperatures, with R^2 values > 0.990, with the exception of the No Treatment (SB) sample dried at 40 °C, where the best fit was the model Page. Because the values of SSE, MSE, and RMSE are much closer to zero, with respect to the logarithmic model, despite the fact that its R^2 is 0.924 and the logarithmic is 0.994, this demonstrated a good data fit. Quequeto et al. [23], Martins et al. [24], Martins et al. [18], and Gasparin et al. [20] found similar values of R^2 > 0.990 in drying Piper aduncuma leaves at 40–60 °C, blackberry leaves at 40–70 °C, Serjania marginata leaves at 40–70 °C, and mint leaves at 30 −70 °C, respectively. However, the model with the best fit to describe the drying kinetics in these investigations was the Midilli model. Similarly, Silva et al. [19] and Da Silva et al. [22] dried Genipa americana leaves at 35–65 °C and boldo leaves at 20–60 °C, respectively, reporting that the model with the best fit was the modified Henderson and Pabis model. A similar behavior was reported by Eneighe et al. [25] on Xymalos monospora leaves at 50–70 °C, indicating that their data fit the Page and modified Page model. The fit to the best model of the drying data observed in medicinal plants is related to the rapid loss of water in the initial stages of the process in this type of leaves, which generates a more pronounced drying curve and is better characterized by the mathematical model logarithmic.

Table 2. Empirical models, constants, and regressive statistical parameters for muña (Minthostachys mollis) drying at 40 °C.

Sample	Model	Statistics				Parameters							
		r^2	SSE	MSE	RMSE								
SB	Midilli	0.425	5.269	0.258	0.499	a	1.085	B	7.473	k	−57.716	n	−5.971
	Logarithmic	0.994	4.117	0.274	0.524	a	0.575	C	1.563	k	0.012		
	Page	0.924	0.073	0.004	0.062	k	51.380	N	51.380				
	Modified Page	0.521	0.003	0.000	0.014	k	2.618	N	−1.036				
	Henderson and Pabis	0.700	0.131	0.009	0.093	a	1.908	K	0.001				
	Wang and Singh	0.597	4.117	0.257	0.507	a	0.006	B	0.000				
	Peleg	0.659	2.616	0.174	0.418	k_1	0.473	k_2	−0.606				
	Lewis	0.465	0.233	0.016	0.125	k	−0.001						
	Fick's second law	0.923	0.0523	0.073	0.042	D_{eff}	3.182×10^{-10}						
BAA	Midilli	0.963	0.114	0.006	0.078	a	−0.585	B	20.399	k	−24.721	n	−3.494
	Logarithmic	0.998	0.001	0.000	0.007	a	0.578	C	1.555	k	0.009		
	Page	0.405	46.497	3.100	1.761	k	51.380	N	51.380				
	Modified Page	0.627	4.539	0.303	0.550	k	2.618	n	−1.028				
	Henderson and Pabis	0.806	0.089	0.006	0.077	a	0.001	k	1.959				
	Wang and Singh	0.556	2.768	0.185	0.430	a	0.006	b	0.000				
	Peleg	0.381	0.284	0.019	0.138	k_1	0.474	k_2	−0.595				
	Lewis	0.704	4.539	0.284	0.533	k	−0.001						
	Fick's second law	0.921	0.146	0.0352	0.077	D_{eff}	3.098×10^{-10}						
B60	Midilli	0.969	0.114	0.006	0.078	a	−0.449	b	27.008	k	−50.981	n	−5.544
	Logarithmic	0.999	0.000	0.000	0.005	a	0.578	c	1.553	k	0.009		
	Page	0.433	45.937	3.062	1.750	k	5.682	n	5.682				
	Modified Page	0.604	4.419	0.295	0.543	k	2.618	n	−1.031				
	Henderson and Pabis	0.790	0.096	0.006	0.080	a	1.946	k	0.001				
	Wang and Singh	0.572	2.719	0.181	0.426	a	0.006	b	0.000				
	Peleg	0.409	0.270	0.018	0.134	k_1	0.473	k_2	−0.599				
	Lewis	0.688	4.419	0.276	0.526	k	−0.001						
	Fick's second law	0.944	0.029	0.230	0.012	D_{eff}	3.075×10^{-10}						

Table 3. Empirical models, constants and regressive statistical parameters for muña (Minthostachys mollis) drying at 50 °C.

Sample	Model	Statistics				Parameters							
		r^2	SSE	MSE	RMSE								
SB	Midilli	0.792	0.058	0.010	0.088	a	16.218	b	−1.564	k	−13.986	n	−3.666
	Logarithmic	1.000	0.000	0.000	0.003	a	0.561	c	1.572	k	0.024		
	Page	0.772	22.841	3.263	1.806	k	43.649	n	43.649				
	Modified Page	0.545	4.616	0.474	0.674	k	2.618	n	−0.885				
	Henderson and Pabis	0.698	0.085	0.012	0.110	a	0.001	k	1.937				
	Wang and Singh	0.772	1.738	0.248	0.498	a	0.011	b	0.000				
	Peleg	0.958	5.656	0.808	0.899	k_1	−8.129	k_2	−0.538				
	Lewis	0.589	2.474	0.309	0.556	k	−0.003						
	Fick's second law	0.872	1.496	0.262	0.991	D_{eff}	6.195×10^{-10}						
BAA	Midilli	0.849	0.051	0.007	0.081	a	0.330	b	−17.883	k	−12.486	n	−1.413
	Logarithmic	0.990	0.003	0.001	0.024	a	0.012	c	1.528	k	0.012		
	Page	0.506	24.891	3.556	1.886	k	42.657	n	42.657				
	Modified Page	0.753	5.520	0.566	0.737	k	2.618	n	−0.858				
	Henderson and Pabis	0.885	0.039	0.006	0.074	a	0.001	k	2.059				
	Wang and Singh	0.486	2.008	0.287	0.536	a	0.013	b	0.000				
	Peleg	0.484	0.174	0.025	0.158	k_1	0.467	k_2	−0.583				
	Lewis	0.789	3.101	0.388	0.623	k	−0.003						
	Fick's second law	0.898	0.957	0.168	0.205	D_{eff}	4.646×10^{-10}						
B60	Midilli	0.809	0.061	0.008	0.088	a	1.273	b	−0.459	k	−15.893	n	−2.460
	Logarithmic	0.995	0.002	0.000	0.017	a	0.613	c	1.545	k	0.013		
	Page	0.561	24.426	3.489	1.868	k	6.561	n	6.561				
	Modified Page	0.714	5.312	0.546	0.724	k	2.618	n	−0.865				
	Henderson and Pabis	0.856	0.046	0.007	0.081	a	0.001	k	2.033				
	Wang and Singh	0.567	1.955	0.279	0.528	a	0.012	b	0.000				
	Peleg	0.539	0.148	0.021	0.145	k_1	0.468	k_2	−0.588				
	Lewis	0.752	2.955	0.369	0.608	k	−0.003						
	Fick's second law	0.866	0.649	0.109	0.352	D_{eff}	4.459×10^{-10}						

Table 4. Empirical models, constants, and regressive statistical parameters for muña (Minthostachys mollis) drying at 60 °C.

Sample	Model	Statistics				Parameters							
		r^2	SSE	MSE	RMSE								
SB	Midilli	0.628	0.098	0.016	0.123	a	0.020	b	−16.572	k	−19.213	n	−1.645
	Logarithmic	0.995	0.001	0.000	0.016	a	0.558	c	1.570	k	0.031		
	Page	0.868	19.703	3.284	1.812	k	21.007	n	21.007				
	Modified Page	0.521	4.015	0.478	0.677	k	2.618	n	−0.833				
	Henderson and Pabis	0.672	0.087	0.014	0.120	a	0.002	k	2.064				
	Wang and Singh	0.786	1.587	0.265	0.514	a	0.012	b	0.000				
	Peleg	0.854	0.039	0.006	0.080	k_1	0.470	k_2	−0.615				
	Lewis	0.567	2.193	0.313	0.560	k	−0.003						
	Fick's second law	0.931	0.037	0.0246	0.084	D_{eff}	7.744×10^{-10}						
BAA	Midilli	0.976	0.007	0.002	0.041	a	0.002	b	−15.807	k	−31.810	n	−2.262
	Logarithmic	0.997	0.001	0.000	0.013	a	0.569	c	1.565	k	0.026		
	Page	0.801	20.030	3.338	1.827	k	88.354	n	88.354				
	Modified Page	0.565	4.153	0.495	0.688	k	2.618	n	−0.852				
	Henderson and Pabis	0.713	0.079	0.013	0.114	a	0.001	k	1.950				
	Wang and Singh	0.798	1.653	0.275	0.525	a	0.012	b	0.000				
	Peleg	0.968	5.599	0.933	0.966	k_1	−8.479	k_2	−0.530				
	Lewis	0.602	2.291	0.327	0.572	k	−0.003						
	Fick's second law	0.946	0.358	0.029	0.071	D_{eff}	7.357×10^{-10}						
B60	Midilli	0.859	0.042	0.007	0.081	a	0.628	b	0.521	k	−14.952	n	−2.068
	Logarithmic	0.988	0.004	0.001	0.027	a	0.636	c	1.524	k	0.012		
	Page	0.840	22.004	3.667	1.915	k	21.007	n	21.007				
	Modified Page	0.776	5.014	0.596	0.756	k	2.618	n	−0.833				
	Henderson and Pabis	0.893	0.032	0.005	0.073	a	0.002	k	2.064				
	Wang and Singh	0.505	1.869	0.312	0.558	a	0.015	b	0.000				
	Peleg	0.789	5.922	0.987	0.994	k_1	−7.390	k_2	−0.514				
	Lewis	0.798	2.838	0.405	0.637	k	−0.003						
	Fick's second law	0.969	0.682	0.032	0.458	D_{eff}	7.583×10^{-10}						

3.3. Diffusion Coefficient, Thermodynamic Properties and Activation Energy

3.3.1. Water Diffusion Coefficient

In the traditional method to study the transfer of mass in a transient state during the drying of foods, the equation of Fick's second law is used since, from it, the diffusion coefficient of water (D_{eff}) can be determined. The D_{eff} values obtained for each sample at different drying temperatures are presented in Table 5. The diffusivity values of water increased as the drying temperature increased, so values between 3.098 and 7.744 $\times 10^{-10}$ were obtained. m^2/s in the range of 40–60 °C. These values were similar to those reported by Doymaz et al. [26] and Kaya and Aydin [27] in mint leaves drying 0.307–1.941 $\times 10^{-8}$ m^2/s between 35–60 °C and 1.975–6.172 $\times 10^{-9}$ m^2/s between 35–55 °C, respectively. Kaya and Aydin [27] recorded values in nettle leaves between 1.744–4.992 $\times 10^{-9}$ m^2/s between 35–55 °C, while Doymaz et al. [28] recorded values in parsley leaves, which were reported as 0.900–2.337 $\times 10^{-9}$ m^2/s, involving drying with hot air between 50–70 °C. Therefore, the values found agree with the water diffusivity data during the drying of the different types of leaves. At low diffusion coefficient, higher temperatures can be used to speed up the drying process, as long as it is ensured that the temperature does not damage the material. On the other hand, if the diffusion coefficient is high, lower temperatures can be used to dry the material more gently and preserve its quality. The diffusion coefficient is important in the drying process because it helps to improve the efficiency of the drying process and to preserve the quality of the material.

Table 5. Effective diffusivity and thermodynamic parameters of drying muña leaves.

Sample	Temperature (°C)	Effective Diffusivity ($D_{eff} \times 10^{-10}$ m^2/s)	Δh (kJ/mol)	Δs (kJ/mol × K)	ΔG (kJ/mol)	Activation Energy (kJ/mol)	R^2
SB	40	3.182 ± 0.049	37.332	−0.229	109.288		
	50	6.195 ± 0.040	37.249	−0.230	111.587	39.935	0.929
	60	7.744 ± 0.012	37.166	−0.230	113.889		
BAA	40	3.098 ± 0.162	37.329	−0.228	108.955		
	50	4.646 ± 0.854	36.992	−0.229	111.252	39.315	0.992
	60	7.357 ± 0.014	36.909	−0.230	113.487		
B60	40	3.075 ± 0.035	37.075	−0.229	108.957		
	50	4.459 ± 0.475	36.984	−0.229	111.305	39.678	0.922
	60	7.583 ± 0.014	36.709	−0.230	113.551		

3.3.2. Thermodynamic Properties

Considering the thermodynamic properties (specific enthalpy, specific entropy, and Gibbs free energy), it was observed that the enthalpy values decreased from 37.332 to 36.909 kJ/mol with increasing temperature (Table 5). Therefore, the higher the temperature, the less specific energy is required for drying. The entropy presented a similar behavior; that is, it decreased from −0.229 to −0.236 kJ/mol·K with increasing temperatures. Negative entropy values were attributed to chemical adsorption and/or structural modifications of the adsorbent [29]. The Gibbs free energy increased with the increase in drying temperature, which indicates that said drying was not spontaneous under the conditions of this work. This means that an endergonic reaction took place; therefore, it needed the addition of energy in the medium in which the product was found for the drying to occur. The Gibbs free energy values found for the pretreated leaves were between 108.955 and 113.889 kJ/mol between 40 and 60 °C. The values found for Δh, Δs, and ΔG were lower than those reported by Quequeto et al. [23] and da Silva et al. [22] in Piper aduncum leaves (15.200 kJ/mol, −0.303 kJ/mol·K and 147.935 kJ/mol) and bay leaves (53.038 kJ/mol, −0.451 kJ/mol·K and 156.587 kJ/mol) dried at 40–60 °C, respectively, although the Δh value was higher compared to bay leaves. The Gibbs free energy indicates the availability of energy to carry out a reaction, and it can be used to determine if the drying process is taking place under the right conditions. Enthalpy and entropy are important to predict the behavior of dried

leaves under different conditions, such as humidity and temperature, and they can be used to control the quality of the final product. These parameters are important to ensure the efficiency of the drying process, to select the operating conditions, to control the quality of the final product, and to optimize the design of the process.

3.3.3. Activation Energy

From the slope of the straight line described by the Arrhenius equation, the activation energy for the different treatments was calculated (Table 5). These results are similar to those reported by Lemus-Mondaca et al. [8], Bensebia and Allia [21], Doymaz [26] and Doymaz et al. [28] (39.910, 66.300, 62.960, 35.050, and 43.920 kJ/mol, in stevia, mint, bay, dill, and parsley leaves, respectively). The data did not present a definite trend, since they are similar to each other with the increase in temperature. The activation energy, Gibbs free energy, enthalpy, and entropy in leaf drying can be used to design and optimize the drying process. The activation energy is essential to choose the right temperature and time to dry the leaves efficiently. If the activation energy is high, the drying process will be slow and expensive, while, if it is too low, it can cause a decrease in the quality of the sheets.

4. Conclusions

The logarithmic model was found to have the best statistical fit for the experimental data of muña leaves drying kinetics, with and without pre-treatment, at temperatures of 40, 50, and 60 °C. As the drying air temperature increased, the time required to remove water from the leaves decreased, and the effective diffusion coefficient increased. The relationship between the effective diffusion coefficient and the drying air temperature enabled the calculation of the activation energy. The increase in drying air temperature reduced the enthalpy and specific entropy values, while the Gibbs free energy values displayed an inverse behavior. These models can help to demonstrate the drying behavior and to determine the drying time required for equipment design.

Author Contributions: Conceptualization, A.E.-S. and R.J.S.-P.; methodology, R.J.S.-P., D.K.M.-M. and A.E.-S.; software, R.J.S.-P.; validation, R.J.S.-P. and A.E.-S.; research, R.J.S.-P., D.K.M.-M. and A.E.-S.; resources, R.J.S.-P.; data curation, R.J.S.-P.; writing—original draft preparation, A.E.-S. and R.J.S.-P.; writing—reviewing and editing, R.J.S.-P. and A.E.-S.; visualization, R.J.S.-P. All authors have read and agreed to the published version of the manuscript.

Institutional Review Board Statement: Not applicable.

Informed Consent Statement: Not applicable.

Data Availability Statement: Not applicable.

Conflicts of Interest: The authors declare no conflict of interest.

References

1. Cano, C.; Bonilla, P.; Roque, M.; Ruiz, J. Actividad antimicótica in vitro y metabolitos del aceite esencial de las hojas de Minthostachys mollis (muña). *Revista Peruana Medicina Experimental Y Salud Pública* **2008**, *25*, 298–301.
2. PromPerú—Comisión De Promoción Del Perú Para La Exportación Y El Turismo. Súper Muña. 2021. Available online: https://peru.info/es-pe/superfoods/detalle/super-muna (accessed on 15 August 2022).
3. Dalia, P.P.; Park, J.S.; Moscoso, M.R.; Salazar-Granara, A. Diferencias en la presencia de alcaloides y fenoles de cinco muestras de muña de expendio informal procedentes de mercados populares en Lima-Perú. Horizonte Médico. *Horiz. Médico* **2018**, *18*, 25–29.
4. Aguirre Tipismana, L.G. Consumo De Plantas Medicinales En Usuarios Del Centro Integral Del Adulto Mayor De La Molina. USMP. 2017. Available online: https://repositorio.usmp.edu.pe/handle/20.500.12727/4398 (accessed on 25 August 2022).
5. Instituto Nacional De Estadística E Informática–Perú (INEI). Estimaciones Y Proyecciones De Población, 1950–2050. Boletín De Análisis Demográfico, N° 36, 2017. Available online: http://190.102.131.45/epidemiologia/pdf/interes_2.pdf (accessed on 10 July 2022).

6.   Roersch, C. Medicinal plants in the Dominican Republic and their possible role in public health care. In Proceedings of the XXIX International Horticultural Congress on Horticulture: Sustaining Lives, Livelihoods and Landscapes (IHC2014): V World Congress on Medicinal and Aromatic Plants and International Symposium on Plants, as Factories of Natural Substances, Edible and Essential Oils, Brisbane, Australia, 17 August 2014; Volume 1125, pp. 249–254.

7.   Fuertes, C.; Murguía, Y. Estudio comparativo del aceite esencial de Minthostachys mollis (Kunth) Griseb "muña" de tres regiones peruanas por cromatografía de gases y espectrometría de masas. *Rev. Cienc. E Investig.* **2001**, *4*, 23–39. [CrossRef]

8.   Lemus-Mondaca, R.; Vega-Gálvez, A.; Moraga, N.O.; Astudillo, S. Dehydration of S tevia rebaudiana Bertoni Leaves: Kinetics, Modeling and Energy Features. *J. Food Process. Preserv.* **2015**, *39*, 508–520. [CrossRef]

9.   Dorneles, L.D.N.S.; Goneli, A.L.D.; Cardoso, C.A.L.; da Silva, C.B.; Hauth, M.R.; Oba, G.C.; Schoeninger, V. Effect of air temperature and velocity on drying kinetics and essential oil composition of Piper umbellatum L. leaves. *Ind. Crops Prod.* **2019**, *142*, 111846. [CrossRef]

10. Przeor, M.; Flaczyk, E.; Beszterda, M.; Szymandera-Buszka, K.E.; Piechocka, J.; Kmiecik, D.; Szczepaniak, O.; Kobus-cisowska, J.; Jarzębski, M.; Tylewicz, U. Air-drying temperature changes the content of the phenolic acids and flavonols in white mulberry (*Morus alba* L.) leaves. *Ciência Rural* **2019**, *49*. [CrossRef]

11. Khodja, Y.K.; Dahmoune, F.; Madani, K.; Khettal, B. Conventional method and microwave drying kinetics of *Laurus nobilis* leaves: Effects on phenolic compounds and antioxidant activity. *Braz. J. Food Technol.* **2020**, *23*. [CrossRef]

12. Bosco, D.; Roche, L.A.; Della Rocca, P.A.; Mascheroni, R.H. Osmodehidrocongelación de batata fortificada con zinc y calcio. *Innotec* **2018**, 23–31. [CrossRef]

13. Fernando, J.A.K.M.; Amarasinghe, A.D.U.S. Drying kinetics and mathematical modeling of hot air drying of coconut coir pith. *SpringerPlus* **2016**, *5*, 807. [CrossRef]

14. Babu, A.K.; Kumaresan, G.; Raj, V.A.A.; Velraj, R. Review of leaf drying: Mechanism and influencing parameters, drying methods, nutrient preservation, and mathematical models. *Renew. Sustain. Energy Rev.* **2018**, *90*, 536–556. [CrossRef]

15. Rocha, R.P.D.; Melo, E.D.C.; Corbín, J.B.; Berbert, P.A.; Donzeles, S.M.; Tabar, J.A. Cinética del secado de tomillo. *Rev. Bras. Eng. Agrícola E Ambient.* **2012**, *16*, 675–683. [CrossRef]

16. Bahammou, Y.; Tagnamas, Z.; Lamharrar, A.; Idlimam, A. Thin-layer solar drying characteristics of Moroccan horehound leaves (*Marrubium vulgare* L.) under natural and forced convection solar drying. *Sol. Energy* **2019**, *188*, 958–969. [CrossRef]

17. Jideani, V.A.; Mpotokwana, S.M. Modeling of water absorption of Botswana bambara varieties using Peleg's equation. *J. Food Eng.* **2009**, *92*, 182–188. [CrossRef]

18. Martins, E.A.; Lage, E.Z.; Goneli, A.L.; Hartmann Filho, C.P.; Lopes, J.G. Cinética de secagem de folhas de timbó (*Serjania marginata* Casar). *Rev. Bras. Eng. Agrícola E Ambient.* **2015**, *19*, 238–244. [CrossRef]

19. Silva, L.A.; Resende, O.; Virgolino, Z.Z.; Bessa, J.F.V.; Morais, W.A.; Vidal, V.M. Cinética de secagem e difusividade efetiva em folhas de jenipapo (*Genipa americana* L.). *Rev. Bras. De Plantas Med.* **2015**, *17*, 953–963. [CrossRef]

20. Gasparin, P.P.; Christ, D.; Coelho, S.R.M. Secagem de folhas *Mentha piperita* em leito fixo utilizando diferentes temperaturas e velocidades de ar. *Rev. Ciênc. Agron.* **2017**, *48*, 242–250.

21. Bensebia, O.; Allia, K. Drying and extraction kinetics of rosemary leaves: Experiments and modeling. *J. Essent. Oil-Bear. Plants* **2015**, *18*, 99–111. [CrossRef]

22. Da Silva, N.C.B.; dos Santos, S.G.; da Silva, D.P.; Silva, I.L.; Rodovalho, R.S. Drying kinetics and thermodynamic properties of boldo (*Plectranthus barbatus* Andrews) leaves. *Científica* **2019**, *47*, 1–7. [CrossRef]

23. Quequeto, W.D.; Siqueira, V.C.; Mabasso, G.A.; Isquierdo, E.P.; Leite, R.A.; Ferraz, L.R.; Hoscher, R.H.; Schoeninger, V.; Jordan, R.A.; Goneli, A.L.D.; et al. Mathematical modeling of thin-layer drying kinetics of *Piper aduncum* L. leaves. *J. Agric. Sci.* **2019**, *11*, 225–235. [CrossRef]

24. Martins, E.A.; Goneli, A.L.; Goncalves, A.A.; Hartmann Filho, C.P.; Siqueira, V.C.; Oba, G.C. Drying kinetics of blackberry leaves. *Rev. Bras. Eng. Agrícola E Ambient.* **2018**, *22*, 570–576. [CrossRef]

25. Eneighe, S.A.; Dzelagha, F.B.; Nde, D.B. Production of an herbal green tea from ambang (*Xymalos monospora*) leaves: Influence of drying method and temperature on the drying kinetics and tea quality. *J. Food Sci. Technol.* **2020**, *57*, 3381–3389. [CrossRef]

26. Doymaz, I. Thin-layer drying behaviour of mint leaves. *J. Food Eng.* **2006**, *74*, 370–375. [CrossRef]

27. Kaya, A.; Aydın, O. An experimental study on drying kinetics of some herbal leaves. *Energy Convers. Manag.* **2009**, *50*, 118–124. [CrossRef]

28. Doymaz, İ.; Tugrul, N.; Pala, M. Drying characteristics of dill and parsley leaves. *J. Food Eng.* **2006**, *77*, 559–565. [CrossRef]

29. Moreira, R.; Chenlo, F.; Torres, M.D.; Vallejo, N. Thermodynamic analysis of experimental sorption isotherms of loquat and quince fruits. *J. Food Eng.* **2008**, *88*, 514–521. [CrossRef]